

## Ruthenium(II) Complexes Containing Bis(2-(diphenylphosphino)phenyl) Ether and Their Catalytic Activity in Hydrogenation Reactions

Ramalingam Venkateswaran,<sup>†</sup> Joel T. Mague,<sup>‡</sup> and Maravanji S. Balakrishna\*<sup>†</sup>

Phosphorus Laboratory, Department of Chemistry, Indian Institute of Technology Bombay, Mumbai 400 076, India, and Department of Chemistry, Tulane University, New Orleans, Louisiana 70118

Received September 20, 2006

The half-sandwich complexes  $[(\eta^5\text{-C}_5\text{H}_5)\text{RuCl}(\text{DPEphos})]$  (**1**) and  $[(\eta^6\text{-}p\text{-cymene})\text{RuCl}_2]_2(\mu\text{-DPEphos})$  (**2**) were synthesized by the reaction of bis(2-(diphenylphosphino)phenyl) ether (DPEphos) with a mixture of ruthenium trichloride trihydrate and cyclopentadiene and with  $[(\eta^6\text{-}p\text{-cymene})\text{RuCl}_2]_2$ , respectively. Treatment of DPEphos with *cis*- $[\text{RuCl}_2(\text{dmsO})_4]$  afforded *fac*- $[\text{RuCl}_2(\kappa^3\text{-}P, O, P\text{-DPEphos})(\text{dmsO})]$  (**3**). The dmsO ligand in **3** can be substituted by pyridine, 2,2'-bipyridine, 4,4'-bipyridine, and  $\text{PPh}_3$  to yield *trans, cis*- $[\text{RuCl}_2(\text{DPEphos})(\text{C}_5\text{H}_5\text{N})_2]$  (**4**), *cis, cis*- $[\text{RuCl}_2(\text{DPEphos})(2,2'\text{-bipyridine})]$  (**5**), *trans, cis*- $[\text{RuCl}_2(\text{DPEphos})(\mu\text{-}4,4'\text{-bipyridine})]_n$  (**6**), and *mer, trans*- $[\text{RuCl}_2(\kappa^3\text{-}P, P, O\text{-DPEphos})(\text{PPh}_3)]$  (**7**), respectively. Refluxing  $[(\eta^6\text{-}p\text{-cymene})\text{RuCl}_2]_2$  with DPEphos in moist acetonitrile leads to the elimination of the *p*-cymene group and the formation of the octahedral complex *cis, cis*- $[\text{RuCl}_2(\text{DPEphos})(\text{H}_2\text{O})(\text{CH}_3\text{CN})]$  (**8**). The structures of the complexes **1–5**, **7**, and **8** are confirmed by X-ray crystallography. The catalytic activity of these complexes for the hydrogenation of styrene is studied.

### Introduction

The chemistry of  $\text{Ru}^{\text{II}}$  complexes incorporating phosphorus donor ligands has received considerable attention in recent years since the discovery of Noyori's BINAP- $\text{RuX}_2$  catalysts, which developed a practical way to prepare an intermediate for the synthesis of prostaglandin and carbapenam antibiotics,<sup>1</sup> and Grubb's  $\text{L}_2\text{X}_2\text{Ru}=\text{CHR}$  catalysts, leading to impressive development in the field of olefin metathesis.<sup>2</sup>  $\text{Ru}^{\text{II}}$  complexes containing nitrogen donor ligands have acquired considerable significance in supramolecular chemistry,<sup>3</sup> photoredox processes for solar energy conversions, biosensors, and catalysis.<sup>4</sup> Phosphorus-, nitrogen-, and sulfur-

containing ligands such as  $\text{PPh}_3$ , dpmm, dppe, pyridines, and dmsO associated with Ru are well documented,<sup>5</sup> whereas the ruthenium chemistry of bis(2-(diphenylphosphino)phenyl) ether (DPEphos) has not been studied. The large bite angle DPEphos with a relatively rigid diphenyl ether backbone and containing both oxygen and phosphorus donor sites<sup>6</sup> offers different coordination modes through the possibility of behaving as a hemilabile ligand, thereby providing the promise of rich coordination and organometallic chemistry with various metal centers. van Leeuwen and co-workers<sup>7</sup> and others<sup>8</sup> have extensively studied the coordination chemistry and catalytic utility of DPEphos.<sup>9</sup> As part of our research interest,<sup>10</sup> herein we report the syntheses of ruthenium

\* To whom correspondence should be addressed. E-mail: krishna@chem.iitb.ac.in. Fax: +91-22-5172-3480.

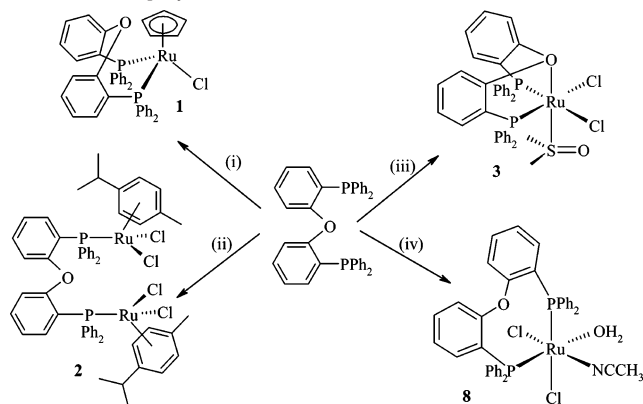
<sup>†</sup> Indian Institute of Technology.

<sup>‡</sup> Tulane University.

- (1) (a) Noyori, R.; Ohkuma, T. *Angew. Chem., Int. Ed.* **2001**, *40*, 40–73. (b) Noyori, R. *Angew. Chem., Int. Ed.* **2002**, *41*, 2008–2022. (c) Mikami, K.; Korenaga, T.; Ohkuma, T.; Noyori, R. *Angew. Chem., Int. Ed.* **2000**, *39*, 3707–3710.
- (2) (a) Grubbs, R. H.; Chang, S. *Tetrahedron* **1998**, *54*, 4413–4450. (b) Trnka, T. M.; Day, M. W.; Grubbs, R. H. *Organometallics* **2001**, *20*, 3845–3847.
- (3) Cronin, L. *Annu. Rep. Prog. Chem., Sect. A: Inorg. Chem.* **2005**, *101*, 348–374.
- (4) (a) Ward, M. D. *Annu. Rep. Prog. Chem., Sect. A: Inorg. Chem.* **2005**, *101*, 649–672. (b) Chelucci, G.; Thummel, R. P. *Chem. Rev.* **2002**, *102*, 3129–3170.

- (5) (a) Fache, F.; Schulz, E.; Tommasino, M. L.; Lemaire, M. *Chem. Rev.* **2000**, *100*, 2159–2231. (b) Tang, W.; Zhang, X. *Chem. Rev.* **2003**, *103*, 3029–3069. (c) Drozdzak, R.; Allaert, B.; Ledoux, N.; Dragutan, I.; Dragutan, V.; Verpoort, F. *Coord. Chem. Rev.* **2005**, *249*, 3055–3074.
- (6) Kamer, P. C. J.; van Leeuwen, P. W. N. M.; Reek, J. N. H. *Acc. Chem. Res.* **2001**, *34*, 895–904.
- (7) (a) Kranenburg, M.; van der Burgt, Y. E. M.; Kamer, P. C. J.; van Leeuwen, P. W. N. M.; Goubitz, K.; Fraanje, J. *Organometallics* **1995**, *14*, 3081–3089. (b) van Haaren, R. J.; Zuidema, E.; Fraanje, J.; Goubitz, K.; Kamer, P. C. J.; van Leeuwen, P. W. N. M.; van Strijdonck, G. P. F. C. R. *Chim.* **2002**, *5*, 431–440. (c) Zuideveld, M. A.; Swennenhuis, B. H. G.; Boele, M. D. K.; Guari, Y.; van Strijdonck, G. P. F.; Reek, J. N. H.; Kamer, P. C. J.; Goubitz, K.; Fraanje, J.; Lutz, M.; Spek, A. L.; van Leeuwen, P. W. N. M. *J. Chem. Soc., Dalton Trans.* **2002**, 2308–2317.

**Scheme 1.** Reactions of DPEphos with (i) RuCl<sub>3</sub> and Cp in Ethanol, (ii) [RuCl<sub>2</sub>(*p*-cymene)]<sub>2</sub> in CH<sub>2</sub>Cl<sub>2</sub>, (iii) *cis*-[RuCl<sub>2</sub>(dmsO)<sub>4</sub>] in CH<sub>2</sub>Cl<sub>2</sub>, and (iv) [RuCl<sub>2</sub>(*p*-cymene)]<sub>2</sub> in CH<sub>3</sub>CN



complexes containing DPEphos and studies in the catalytic hydrogenation of styrene.

## Results and Discussion

Treatment of a mixture of DPEphos and cyclopentadiene with ruthenium trichloride affords the half-sandwich complex [( $\eta^5$ -C<sub>5</sub>H<sub>5</sub>)RuCl(DPEphos)] (**1**) in good yield (Scheme 1).

The <sup>31</sup>P NMR spectrum of complex **1** shows single resonance at 42.4 ppm. The cyclopentadiene group presents a single resonance at 4.10 ppm in the <sup>1</sup>H NMR spectrum.

- (8) (a) Kim, D.; Park, B.-M.; Yun, J. *Chem. Commun.* **2005**, 1755–1757. (b) Kuang, S.-M.; Cuttell, D. G.; McMillin, D. R.; Fanwick, P. E.; Walton, R. A. *Inorg. Chem.* **2002**, *41*, 3313–3322. (c) Kuang, S.-M.; Fanwick, P. E.; Walton, R. A. *Inorg. Chem.* **2002**, *41*, 405–412. (d) Wilting, J.; Muller, C.; Hewat, A. C.; Ellis, D. D.; Tooke, D. M.; Spek, A. L.; Vogt, D. *Organometallics* **2005**, *24*, 13–15. (e) Pintado-Alba, A.; de la Riva, H.; Nieuwhuyzen, M.; Bautista, D.; Raithby, P. R.; Sparkes, H. A.; Teat, S. J.; López-de-Luzuriaga, J. M.; Lagunas, M. C. *Dalton Trans.* **2004**, 3459–3467.
- (9) (a) van Leeuwen, P. W. N. M.; Kamer, P. C. J.; Reek, J. N. H.; Dierkes, P. *Chem. Rev.* **2000**, *100*, 2741–2769. (b) Ahmed, M.; Seayad, A. M.; Jackstell, R.; Beller, M. *J. Am. Chem. Soc.* **2003**, *125*, 10311–10318. (c) Broutin, P.-E.; Cerna, I.; Campaniello, M.; Leroux, F.; Colobert, F. *Org. Lett.* **2004**, *6*, 4419–4422. (d) Chen, Y.; Zhang, X. P. *J. Org. Chem.* **2003**, *68*, 4432–4438. (e) Csuk, R.; Barthel, A.; Raschke, C. *Tetrahedron* **2004**, *60*, 5737–5750. (f) Gao, G.-Y.; Colvin, A. J.; Chen, Y.; Zhang, X. P. *Org. Lett.* **2003**, *5*, 3261–3264. (g) Kozawa, Y.; Mori, M. *J. Org. Chem.* **2003**, *68*, 3064–3067. (h) Kuwano, R.; Kondo, Y.; Matsuyama, Y. *J. Am. Chem. Soc.* **2003**, *125*, 12104–12105. (i) Ogasawara, M.; Ikeda, H.; Nagano, T.; Hayashi, T. *Org. Lett.* **2001**, *3*, 2615–2617. (j) Oh, C. H.; Reddy, V. R. *Tetrahedron Lett.* **2004**, *45*, 5221–5224. (k) Willis, M. C.; Taylor, D.; Gillmore, A. T. *Org. Lett.* **2004**, *6*, 4755–4757. (l) Wolfe, J. P.; Rossi, M. A. *J. Am. Chem. Soc.* **2004**, *126*, 1620–1621.
- (10) (a) Balakrishna, M. S.; Santarsiero, B. D.; Cavell, R. G. *Inorg. Chem.* **1994**, *33*, 3079–3084. (b) Balakrishna, M. S.; Panda, R.; Smith, D. C. J.; Klamann, A.; Nolan, S. P. *J. Organomet. Chem.* **2000**, *599*, 159–165. (c) Balakrishna, M. S.; Abhyankar, R. M.; Walawalker, M. G. *Tetrahedron Lett.* **2001**, *42*, 2733–2734. (d) Balakrishna, M. S.; Teipel, S.; Pinkerton, A. A.; Cavell, R. G. *Inorg. Chem.* **2001**, *40*, 1802–1808. (e) Balakrishna, M. S.; Panda, R.; Mague, J. T. *J. Chem. Soc., Dalton Trans.* **2002**, 4617–4621. (f) Balakrishna, M. S.; Panda, R.; Mague, J. T. *Polyhedron* **2003**, *22*, 587–593. (g) Priya, S.; Balakrishna, M. S.; Mobin, S. M.; McDonald, R. J. *Organomet. Chem.* **2003**, *688*, 227–235. (h) Chandrasekaran, P.; Mague, J. T.; Balakrishna, M. S. *Inorg. Chem.* **2005**, *44*, 7925–7932. (i) Chandrasekaran, P.; Mague, J. T.; Balakrishna, M. S. *Organometallics* **2005**, *24*, 3780–3783. (j) Chandrasekaran, P.; Mague, J. T.; Balakrishna, M. S. *Inorg. Chem.* **2006**, *45*, 5893–5897. (k) Chandrasekaran, P.; Mague, J. T.; Balakrishna, M. S. *Inorg. Chem.* **2006**, *45*, 6678–6683. (l) Punji, B.; Mague, J. T.; Balakrishna, M. S. *Dalton Trans.* **2006**, 1322–1330. (m) Punji, B.; Ganesamoorthy, C.; Balakrishna, M. S. *J. Mol. Catal. A: Chem.* **2006**, *259*, 78–83. (n) Punji, B.; Mague, J. T.; Balakrishna, M. S. *J. Organomet. Chem.* **2006**, *691*, 4265–4272.

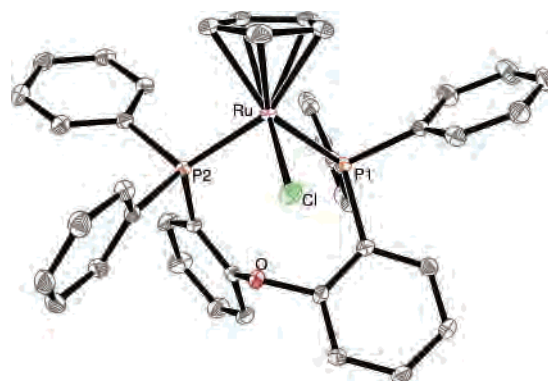


**Figure 1.** Molecular structure of complex **1**. Thermal ellipsoids are drawn at 50% probability level. Hydrogen atoms have been omitted for clarity.

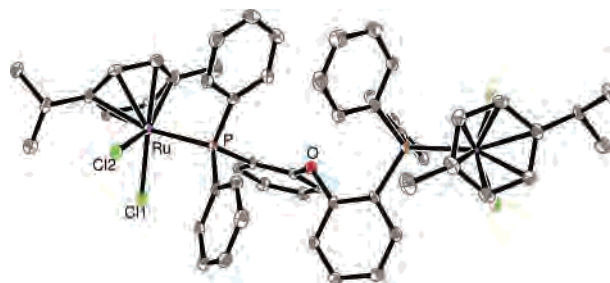


**Figure 2.** Molecular structure of complex **2**. Thermal ellipsoids are drawn at 50% probability level. Hydrogen atoms have been omitted for clarity.

The mass spectrum (EI) and microanalysis supports the structure, which is further confirmed by single-crystal X-ray crystallography. The Ru<sup>II</sup> center adopts distorted tetrahedral geometry in which the P1–Ru–P2, P1–Ru–Cl, and P2–Ru–Cl bond angles are 96.14(2)°, 88.19(2)°, and 95.52(2)°, respectively. The Ru–P bond distances are 2.294(1) and 2.321(1) Å, and the Ru–C bond distances range from 2.192(2) to 2.222(2) Å with an average bond distance of 2.206(1) Å, values which are consistent with the literature.<sup>11</sup> The bite angle of DPEphos in complex **1** is 96.14°, which is 5.86° less than the natural bite angle ( $\beta_n = 102^\circ$ )<sup>6</sup> (Figure 1).

The reaction of DPEphos with [RuCl<sub>2</sub>( $\eta^6$ -*p*-cymene)]<sub>2</sub> in 1:1 molar ratio results in the formation of the binuclear complex [( $\eta^6$ -*p*-cymene)RuCl<sub>2</sub>]<sub>2</sub>( $\mu$ -DPEphos)] (**2**). The <sup>1</sup>H NMR spectrum of **2** shows peaks at 1.16 (d), 1.80 (s), 2.87 (s, br), 4.79 (d), and 5.00 (d) ppm corresponding to the *p*-cymene group. The <sup>31</sup>P NMR spectrum shows single resonance at 21.3 ppm. The structure of the complex **2** was confirmed by single-crystal X-ray crystallography, which shows that the molecule possesses crystallographically imposed centrosymmetry. The Ru–C bond distances range from 2.177(3) to 2.256(3) Å with an average bond distance of 2.215(3) Å and the Ru–P bond distance is 2.3706(10) Å. The Cl1–Ru–Cl2, Cl1–Ru–P, and Cl2–Ru–P bond angles of 88.67(3)°, 90.06(3)°, and 85.04(3)° are in accordance with the literature<sup>12</sup> (Figure 2).

The reaction of *cis*-[RuCl<sub>2</sub>(dmsO)<sub>4</sub>] with DPEphos affords exclusively *fac*-[RuCl<sub>2</sub>( $\kappa^3$ -*P,O,P*-DPEphos)(dmsO)] (**3**) in

(11) Bruce, M. I.; Skelton, B. W.; White, A. H.; Zaitseva, N. N. *J. Organomet. Chem.* **2002**, *650*, 141–150.

(12) Jensen, S. B.; Rodger, S. J.; Spicer, M. D. *J. Organomet. Chem.* **1998**, *556*, 151–158.

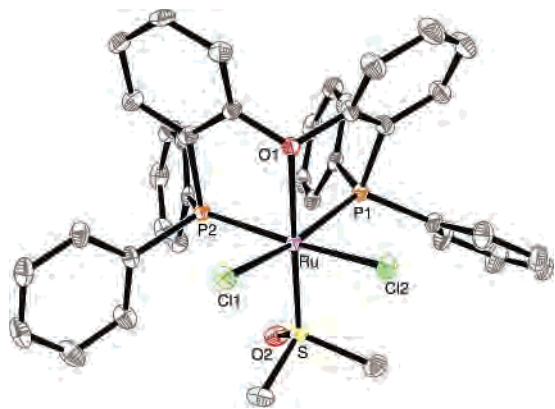


**Figure 3.** Molecular structure of complex **3**. Thermal ellipsoids are drawn at 50% probability level. Hydrogen atoms and uncoordinated solvent molecules have been omitted for clarity.

good yield, irrespective of the stoichiometry and reaction conditions. The  $^{31}\text{P}$  NMR spectrum of complex **3** exhibits a singlet at 45.2 ppm and suggests that both the P atoms are in the same environment either cis to each other and trans to chlorides or mutually trans to each other. Proton NMR displays a singlet at 2.91 ppm corresponding to the methyl protons present in the coordinated dmsoligand. The (EI) mass spectrum displays the isotopic pattern for ruthenium with a molecular ion peak at  $m/z$  752.96  $[\text{M} - \text{Cl}]^+$ . The structure of complex **3** was confirmed by the single-crystal X-ray diffraction study. In the molecular structure of **3**, DPEphos binds to ruthenium in the fac orientation with the  $\kappa^3\text{-P,O,P}$  mode of coordination in which the two phosphorus centers are in cis positions and trans to the chlorides with one dmsoligand (S-donor) coordinating trans to the oxygen atom. The geometry around the ruthenium center is distorted octahedral, as confirmed by  $\text{P1-Ru-Cl1}$ ,  $\text{P1-Ru-S}$ , and  $\text{O-Ru-S}$  bond angles of  $164.45(3)^\circ$ ,  $97.53(3)^\circ$ , and  $178.89(5)^\circ$ , respectively. The bite angle of DPEphos in complex **3** ( $99.16(3)^\circ$ ) is  $2.8^\circ$  less than the natural bite angle value ( $102^\circ$ ).<sup>6</sup> Both Ru–P and Ru–Cl bond lengths are comparable to those for analogous compounds recorded in the literature.

The  $\text{Ru}^{\text{II}}$  complex **3** undergoes substitution reaction with 2 equiv of pyridine to yield *trans,cis*- $[\text{RuCl}_2(\text{DPEphos})(\text{C}_5\text{H}_5\text{N})_2]$  (**4**) in moderate yield. The  $^{31}\text{P}$  NMR spectrum of complex **4** presents a broad single resonance at 38.0 ppm in room temperature and becomes sharp at  $-50^\circ\text{C}$ . The mass spectrum of complex **4** shows a fragment ion peak corresponding to  $[\text{M} - \text{C}_5\text{H}_5\text{N}\cdot\text{Cl}]^+$  at  $m/z$  754.03 with the appropriate isotopic pattern. It is evident from the molecular structure that in the formation of **4**, the *cis*- $[\text{RuCl}_2]$  unit has isomerized to the *trans* geometry and the coordinated oxygen of DPEphos has been displaced. Although no detailed mechanistic information is available, it is tempting to speculate that the initial step in the substitution reaction is replacement of the coordinated oxygen of the DPEphos by the first pyridine ligand. The two phosphorus atoms occupy *cis* positions and are mutually *trans* to the N-donors, whereas

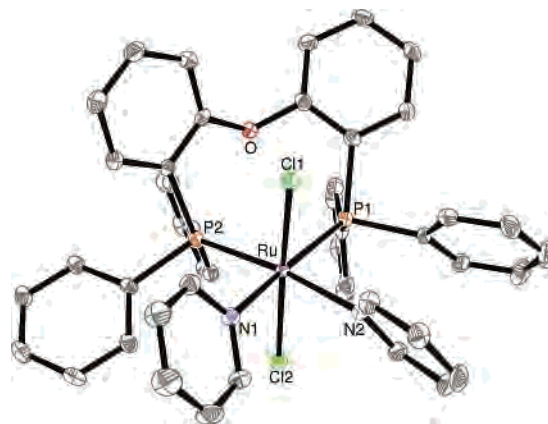
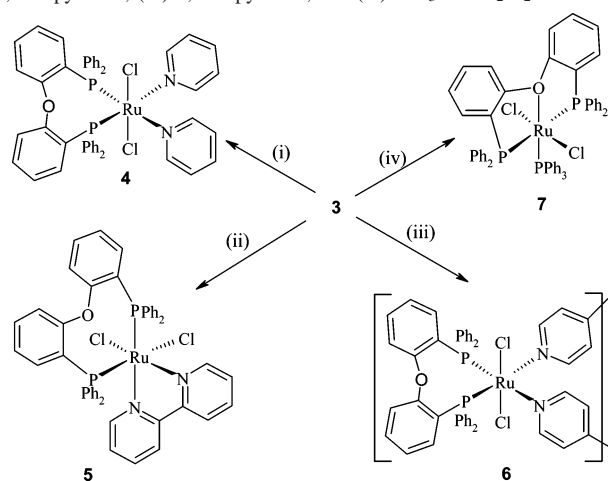


**Figure 4.** Molecular structure of complex **4**. Thermal ellipsoids are drawn at 50% probability level. Hydrogen atoms and uncoordinated solvent molecules have been omitted for clarity.

**Scheme 2.** Reactions of **3** with (i) Pyridine(2 equiv), (ii) 2,2'-Bipyridine, (iii) 4,4'-Bipyridine, and (iv)  $\text{PPh}_3$  in  $\text{CH}_2\text{Cl}_2$



the chlorides are in *trans* positions. The  $\text{P1-Ru-P2}$ ,  $\text{P1-Ru-N1}$ ,  $\text{Cl1-Ru-Cl2}$ , and  $\text{Cl1-Ru-P1}$  bond angles are  $96.09(3)^\circ$ ,  $169.57(7)^\circ$ ,  $174.34(3)^\circ$ , and  $85.72(3)^\circ$ , respectively, and the  $\text{P1-Ru-P2}$  bond angle ( $99.16(3)^\circ$ ) is  $3.09^\circ$  less than that in complex **3**. The Ru–P bond distances of complex **4** are slightly longer (by  $0.02 \text{ \AA}$ ) with respect to those in complex **3**. The Ru–N bond distances are  $2.164(3)$  and  $2.185(3) \text{ \AA}$ , which are slightly longer than the literature values reported for analogous complexes (Figure 4).<sup>14</sup>

The reaction of complex **3** with 1 equiv of 2,2'-bipyridine gives the mononuclear ruthenium complex *cis,cis*- $[\text{RuCl}_2(\text{DPEphos})(2,2'\text{-bipyridine})]$  (**5**) in good yield. The  $^{31}\text{P}$  NMR spectrum of complex **5** displays two doublets centered at 31.0 and 37.0 ppm with a  $^2J_{\text{PP}}$  value of 32.4 Hz which indicates that the two phosphorus atoms are nonequivalent. This implies that one phosphorus is *trans* to Cl and that the other is *trans* to an N atom of 2,2'-bipyridine. Therefore, *cis,cis* is the only possible isomer for the complex **5** as shown in Scheme 2. The mass spectrum of the complex **5** supports the suggested structure, which shows a molecular ion peak at  $m/z$  831.06  $[\text{M} - \text{Cl}]^+$ .

(13) Queiroz, S. L.; Batista, A. A.; Oliva, G.; Gambardella, M. T. P.; Santos, R. H. A.; MacFarlane, K. S.; Rettig, S. J.; James, B. R. *Inorg. Chim. Acta* **1998**, *267*, 209–221.

(14) Baratta, W.; Herdtweck, E.; Siega, K.; Toniutti, M.; Rigo, P. *Organometallics* **2005**, *24*, 1660–1669.



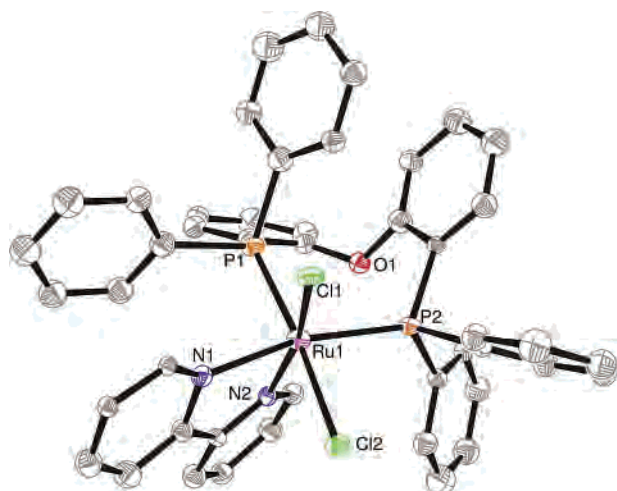


**Figure 5.** Molecular structure of complex **5**. Thermal ellipsoids are drawn at 50% probability level. Hydrogen atoms and uncoordinated solvent molecules have been omitted for clarity.

The structure of the complex **5** was confirmed by X-ray crystallography, which shows the presence of two isostructural molecules present in the asymmetric unit and the Ru center is in a distorted octahedral geometry. The bond parameters of both the molecules differ slightly. The Ru1–Cl1, Ru1–Cl2, Ru1–P1, Ru1–P2, and Ru1–N1 bond distances of 2.392(4), 2.451(4), 2.299(4), 2.332(4), and 2.122(14) Å, respectively, are comparable to complex **4**, whereas the Ru1–N2 bond distance is shorter by 0.1 Å. The bite angle of the DPEphos ligand in complex **5** (100.85(14)°) is 1.64° less than the natural bite angle and 4.76° greater than that in complex **4**. The Cl1–Ru1–Cl2 bond angle (88.87(14)°) is 4.83° greater than that in complex **3**, and the N1–Ru1–N2 bond angle is 78.0(4)° (Figure 5).

The reaction of **3** and 4,4'-bipyridine in an equimolar ratio affords the polynuclear complex *trans,cis*-[RuCl<sub>2</sub>(DPEphos)-(μ-4,4'-bipyridine)]<sub>n</sub> (**6**) in quantitative yield. The <sup>31</sup>P NMR spectrum of complex **6** exhibits a singlet at 36.5 ppm which indicates that both the phosphorus atoms are chemically equivalent. The similarity of the phosphorus chemical shifts between complexes **6** and **4** suggests that the Ru center in the former is in much the same environment as that in the latter, leading to the structure proposed in Scheme 2.

Treatment of complex **3** with triphenylphosphine affords the red crystalline solid formulated as *mer,trans*-[RuCl<sub>2</sub>(κ<sup>3</sup>-P,P,O-DPEphos)(PPh<sub>3</sub>)] (**7**) (Figure 6) in good yield. The <sup>31</sup>P NMR spectrum shows a triplet at 54.0 ppm and a doublet centered at 27.2 ppm in the intensity ratio of 1:2 and with a <sup>2</sup>J<sub>PP</sub> value of 29.4 Hz. The low field resonance is assigned to PPh<sub>3</sub> and the latter value to the two phosphorus atoms of DPEphos. The (EI) mass spectrum of complex **7** shows a molecular ion peak at *m/z* 937.07 [M – Cl]<sup>+</sup>. It is evident from the <sup>31</sup>P NMR spectrum that the two phosphorus in DPEphos are equivalent; hence, the phosphorus atoms are mutually *trans* to each other. The PPh<sub>3</sub> group exhibits a very significant downfield shift of 60 ppm due to the presence of the O-donor in the *trans* position. The structure of complex **7** was confirmed by single-crystal X-ray crystallographic

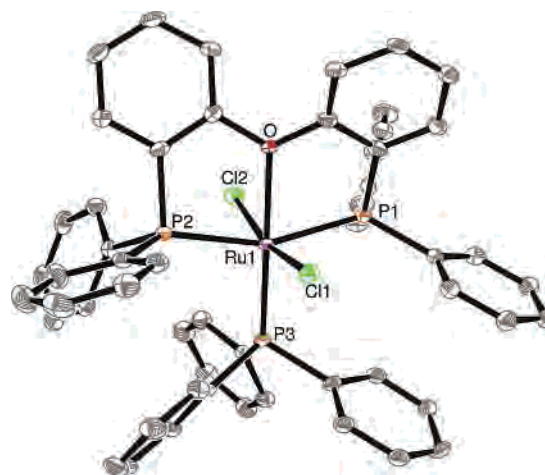


**Figure 6.** Molecular structure of complex **7**. Thermal ellipsoids are drawn at 50% probability level. Hydrogen atoms and uncoordinated solvent molecules have been omitted for clarity.

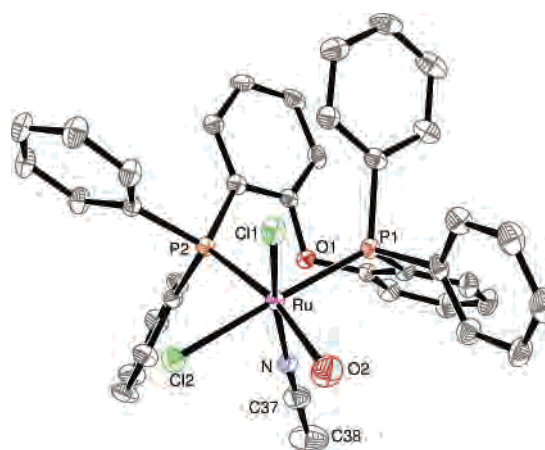


**Figure 7.** Molecular structure of complex **8**. Thermal ellipsoids are drawn at 50% probability level. Hydrogen atoms and uncoordinated solvent molecules have been omitted for clarity.

studies. Although the DPEphos retains the tridentate mode of coordination, the Ru center is transformed to the *mer* isomer. The two chlorides are mutually *trans* to each other, and PPh<sub>3</sub> is *trans* to the oxygen of the DPEphos ligand. The Cl1–Ru1–Cl2, P1–Ru1–P2, P1–Ru1–O, and Cl2–Ru1–P1 bond angles are 166.93(4)°, 158.53(4)°, 79.10(9)°, and 85.77(4)°, respectively, confirming that the geometry of Ru<sup>II</sup> in complex **7** is a highly distorted octahedral. The bite angle of DPEphos in complex **7** is 59.37° higher than that in complex **3**. The bond distance between Ru–P3 (PPh<sub>3</sub>) is 0.1 Å shorter than that of Ru–P1 (DPEphos). The Ru–Cl bond distances (2.4086(12) and 2.3943(12) Å) are 0.03 Å shorter in comparison with those of **3**.

Refluxing DPEphos with [RuCl<sub>2</sub>(η<sup>6</sup>-*p*-cymene)]<sub>2</sub> in a 2:1 molar ratio in moist acetonitrile affords the hydrated mononuclear complex *cis,cis*-[RuCl<sub>2</sub>(DPEphos)(CH<sub>3</sub>CN)(H<sub>2</sub>O)] (**8**) (Figure 7) via elimination of *p*-cymene. The <sup>31</sup>P NMR spectrum of complex **5** shows two doublets centered at 35.3 and 16.9 ppm with a <sup>2</sup>J<sub>PP</sub> value of 31.1 Hz. The <sup>1</sup>H NMR spectrum displays peaks at 1.38 and 2.03 ppm corresponding to coordinated water and acetonitrile molecules. The peaks (as in complex **2**) corresponding to *p*-cymene are not observed in the <sup>1</sup>H NMR, which confirms the elimination

**Table 1.** Crystallographic Information for Complexes 1–4

	1	2	3·3CH <sub>2</sub> Cl <sub>2</sub>	4·2CHCl <sub>3</sub>
formula	C <sub>41</sub> H <sub>33</sub> OP <sub>2</sub> RuCl	C <sub>56</sub> H <sub>56</sub> OP <sub>2</sub> Ru <sub>2</sub> Cl <sub>4</sub>	C <sub>38</sub> H <sub>34</sub> O <sub>2</sub> P <sub>2</sub> RuSCl <sub>2</sub>	C <sub>46</sub> H <sub>38</sub> OP <sub>2</sub> RuN <sub>2</sub> Cl <sub>2</sub>
fw	740.13	1150.89	1043.41	1107.43
cryst syst	monoclinic	orthorhombic	triclinic	monoclinic
space group	<i>P</i> 2 <sub>1</sub> / <i>n</i>	<i>Pbcn</i>	<i>P</i> -1	<i>P</i> 2 <sub>1</sub> / <i>n</i>
<i>a</i> , Å	10.656(1)	22.863(2)	11.4515(9)	10.9687(7)
<i>b</i> , Å	19.077(2)	15.076(1)	13.868(1)	11.9749(8)
<i>c</i> , Å	16.153(2)	14.352(1)	15.372(1)	35.240(2)
α, deg	90	90	92.377(1)	90
β, deg	100.617(2)	90	106.488(1)	94.482(1)
γ, deg	90	90	96.296(1)	90
<i>V</i> , Å <sup>3</sup>	3227.4(6)	4946.9(6)	2320.0(3)	4614.6(5)
<i>Z</i>	4	4	2	4
$\rho_{\text{calc}}$ , g cm <sup>-3</sup>	1.523	1.545	1.494	1.594
$\mu$ (Mo K $\alpha$ ), mm <sup>-1</sup>	0.702	0.932	0.946	0.913
<i>F</i> (000)	1512	2344	1056	2240
cryst size (mm)	0.11 × 0.14 × 0.22	0.04 × 0.13 × 0.14	0.09 × 0.12 × 0.19	0.12 × 0.14 × 0.19
<i>T</i> (K)	100	100	100	100
2 $\theta$ range, deg	1.7–28.3	1.6–28.3	1.4–27.5	1.8–28.3
total no. reflns	28 076	41 946	20 369	40 572
no. of indep reflns	7723 ( <i>R</i> <sub>int</sub> = 0.027)	6077 ( <i>R</i> <sub>int</sub> = 0.058)	10 418 ( <i>R</i> <sub>int</sub> = 0.028)	11 126 ( <i>R</i> <sub>int</sub> = 0.051)
GOF ( <i>F</i> <sup>2</sup> )	1.046	1.111	1.032	1.033
<i>R</i> <sup>a</sup>	0.0301	0.0471	0.0436	0.0489
<i>R</i> <sub>w</sub> <sup>b</sup>	0.0752	0.1103	0.1146	0.1168

$$^a R = \sum ||F_o| - |F_c|| / \sum |F_o|. \quad ^b R_w = \{ [\sum w(F_o^2 - F_c^2) / \sum w(F_o^2)]^{1/2} \}; \quad w = 1 / [\sigma^2(F_o^2) + (xP)^2], \quad \text{where } P = (F_o^2 + 2F_c^2) / 3.$$

of *p*-cymene during the reaction. The mass spectrum exhibits a fragment peak at *m/z* 699.07 corresponding to [M – 2Cl]<sup>+</sup>. The molecular structure of the complex **8**, determined by X-ray crystallography, shows that the geometry of Ru<sup>II</sup> is an octahedral one in which the two phosphorus and chloride members are in *cis* positions. The Cl1–Ru–Cl2, Cl1–Ru–P1, Cl1–Ru–P2, and P1–Ru–P2 bond angles are 85.82(3)°, 87.97(3)°, 104.70(3)°, and 99.22(3)°, respectively, and the bite angle of DPEphos in complex **8** (99.22(3)°) is comparable to that of complex **3**. The Ru–Cl1 (*trans* to N) bond distance is 0.052 Å shorter than the Ru–Cl2 (*trans* to P) bond distance. The Ru–P1 bond distance (2.2921(9) Å) is comparable to that of complex **3**, whereas the bond distance of Ru–P2 is 0.029 Å longer than that of Ru–P1.

The addition of excess DPEphos to complex **3** did not afford the expected product, *trans*-[RuCl<sub>2</sub>(DPEphos)<sub>2</sub>]. Similarly, the reaction of an excess of PPh<sub>3</sub> with complex **7** did not yield *trans,cis*-[RuCl<sub>2</sub>(DPEphos)(PPh<sub>3</sub>)<sub>2</sub>]. This is likely due to the bulkiness of the coordinated DPEphos ligand, which does not allow another bulky ligand to enter into the coordination sphere. In contrast with these observations, the reaction of **3** with 1 equiv of pyridine favors the formation of *trans,cis*-[RuCl<sub>2</sub>(DPEphos)(pyridine)<sub>2</sub>] (**4**) as the predominant product; hence, the complex **4** was prepared in high yield by the 2:1 reaction of pyridine with complex **3**. It indicates that complex **3** allows 2 equiv of less bulky N-donor ligands such as pyridine, 4,4'-bipyridine, or 1 equiv of chelating 2,2'-bipyridine to react with complex **3** (see Tables 1–5 for crystallographic and bond distance and angle information for complexes 1–8).

### Catalytic Hydrogenation of Styrene

The catalytic activity of the complexes 1–8 toward the hydrogenation of styrene was surveyed under the following conditions; [catalyst] = 0.1 mol %, medium = THF, pressure

(H<sub>2</sub>) = 10 atm, and temperature = 70 °C. The conversion rate was periodically monitored by gas chromatography, and the product was confirmed by <sup>1</sup>H NMR spectroscopy. The results are displayed in Table 6. Complete conversions were observed in 4 h for the complexes **3** and **7**, whereas the complexes **1**, **2**, and **8** were near completion after 6, 5, and 4 h, respectively. In the case of complex **7**, after the complete conversion, 1.0 mmol of styrene was again added, the reaction was continued under the same conditions, and complete conversion was observed in 5 h. The slight delay in completion may be due to the partial decomposition of the catalyst. Addition of a drop of mercury to the reaction mixture did not affect the activity of the catalyst, thus indicating that the system is homogeneous. Addition of D<sub>2</sub>O into the reaction mixture did not affect the conversion rate. The <sup>1</sup>H NMR spectrum of the product shows a triplet and a quartet at 1.24 and 2.65 ppm for CH<sub>3</sub> and CH<sub>2</sub> groups of ethylbenzene, respectively, which confirms the absence of deuterium in the product. This also indicates the noninvolvement of protic solvents in the catalytic reactions. Complex **5** shows less conversion (68.8% after 8 h) in comparison with other complexes, suggesting a high stability and resistance to oxidative addition. The polynuclear complex **6** did not show any appreciable activity, presumably due to its poor solubility in THF. The Ru<sup>II</sup> complexes of 1–4, **7**, and **8** are found to be more efficient in the catalytic hydrogenation of styrene under mild conditions as compared with the other catalysts such as [RuHCl(C<sub>6</sub>Me<sub>6</sub>)(PPh<sub>3</sub>)],<sup>15</sup> [RuCl<sub>2</sub>(dppb)<sub>2</sub>],<sup>16</sup> [RuCl(dppb)(μ-Cl)]<sub>2</sub> (dppb = 1,4-bis-(diphenylphosphino)butane,<sup>17</sup> [RuCl<sub>2</sub>(*p*-cymene)(PPh<sub>2</sub>Py)], and [RuCl(*p*-cymene)(PPh<sub>2</sub>Py)][BF<sub>4</sub>].<sup>18</sup>

(15) Bennett, M. A.; Huang, T.-N.; Smith, A. K.; Turney, T. W. *J. Chem. Soc., Chem. Commun.* **1978**, 582–583.

(16) Suarez, T.; Fontal, B.; Medina, H. *J. Mol. Catal.* **1985**, *50*, 355–363.

**Table 2.** Crystallographic Information for Complexes **5**, **7**, and **8**

	<b>5</b>	<b>7</b> ·CHCl <sub>3</sub> ·C <sub>0.5</sub> H <sub>0.5</sub> Cl <sub>2</sub>	<b>8</b> ·CH <sub>2</sub> Cl <sub>2</sub>
formula	C <sub>47</sub> H <sub>38</sub> OP <sub>2</sub> RuN <sub>2</sub> Cl <sub>4</sub>	C <sub>54</sub> H <sub>43</sub> OP <sub>3</sub> RuCl <sub>2</sub>	C <sub>38</sub> H <sub>35</sub> O <sub>2</sub> P <sub>2</sub> RuNCl <sub>2</sub>
fw	951.60	1169.54	854.49
cryst syst	orthorhombic	monoclinic	triclinic
space group	<i>Pca</i> 2 <sub>1</sub>	<i>P</i> 2 <sub>1</sub> / <i>c</i>	<i>P</i> -1
<i>a</i> , Å	26.076(3)	12.252(1)	11.0985(7)
<i>b</i> , Å	9.7320(10)	36.228(4)	12.2786(8)
<i>c</i> , Å	33.932(4)	12.190(1)	15.715(1)
α, deg	90	90	81.440(1)
β, deg	90	108.018(1)	83.965(1)
γ, deg	90	90	81.457(1)
<i>V</i> , Å <sup>3</sup>	8611.0(17)	5145.4(8)	2086.6(2)
<i>Z</i>	8	4	2
ρ <sub>calc</sub> , g cm <sup>-3</sup>	1.468	1.510	1.360
μ (Mo Kα), mm <sup>-1</sup>	0.725	0.802	0.741
<i>F</i> (000)	3872	2374	868
cryst size (mm)	0.05 × 0.08 × 0.22	0.09 × 0.11 × 0.29	0.09 × 0.14 × 0.22
<i>T</i> (K)	100	100	100
2θ range, deg	1.6–25.0	2.1–28.3	1.3–27.9
total no. reflns	15 161	90 001	18 631
no. of indep reflns	10 248 ( <i>R</i> <sub>int</sub> = 0.148)	12 792 ( <i>R</i> <sub>int</sub> = 0.078)	9568 ( <i>R</i> <sub>int</sub> = 0.033)
GOF ( <i>F</i> <sup>2</sup> )	1.093	1.130	1.046
<i>R</i> <sup>a</sup>	0.1050	0.0655	0.0531
<i>R</i> <sub>w</sub> <sup>b</sup>	0.2797	0.1617	0.1350

$$^a R = \sum ||F_o| - |F_c|| / \sum |F_o|. \quad ^b R_w = \{[\sum w(F_o^2 - F_c^2) / \sum w(F_o^2)]^{1/2}\}; \quad w = 1/[\sigma^2(F_o^2) + (xP)^2] \text{ where } P = (F_o^2 + 2F_c^2)/3.$$

**Table 3.** Selected Bond Distances (Å) and Bond Angles (deg) for Complexes **1** and **2**

complex 1				complex 2			
distance		angle		distance		angle	
Ru–Cl	2.4528(6)	Cl–Ru–P1	88.19(2)	Ru–Cl1	2.4102(8)	Cl1–Ru–Cl2	88.67(3)
Ru–P1	2.2937(5)	Cl–Ru–P2	95.52(2)	Ru–Cl2	2.4196(8)	Cl1–Ru–P	90.06(3)
Ru–P2	2.3209(5)	Cl–Ru–C37	149.87(6)	Ru–P	2.3706(10)	Cl1–Ru–C19	122.76(11)
Ru–C37	2.193(2)	Ru–P1–C1	109.73(6)	Ru–C19	2.256(3)	Cl1–Ru–C20	158.91(10)
Ru–C38	2.222(2)	Ru–P1–C7	117.15(6)	Ru–C20	2.214(3)	Cl2–Ru–P	85.04(3)
Ru–C39	2.213(2)	P1–Ru–P2	96.14(2)	Ru–C21	2.177(3)	P–Ru–C19	94.88(10)
Ru–C40	2.211(2)	C18–O–C19	115.52(14)	Ru–C22	2.233(3)	C6–O–C6 <sub>a</sub>	114.3(3)
Ru–C41				Ru–C23	2.206(3)		
				Ru–C24	2.208(3)		

**Table 4.** Selected Bond Distances (Å) and Bond Angles (deg) for Complexes **3–5**

Complex 3			Complex 4			Complex 5					
distance		angle	distance		angle	distance		angle			
Ru–Cl1	2.4321(8)	Cl1–Ru–Cl2	84.04(3)	Ru–Cl1	2.3988(8)	Cl1–Ru–Cl2	174.34(3)	Ru1–Cl1	2.392(4)	Cl1–Ru1–Cl2	88.87(14)
Ru–Cl2	2.4354(8)	Cl1–Ru–S	96.94(3)	Ru–Cl2	2.4433(8)	Cl1–Ru–P1	85.72(3)	Ru1–Cl2	2.451(4)	Cl1–Ru1–P1	88.22(14)
Ru–S	2.1875(8)	Cl1–Ru–P1	164.45(3)	Ru–N1	2.164(3)	Cl1–Ru–P2	94.58(3)	Ru1–N1	2.122(14)	Cl1–Ru1–P2	94.04(14)
Ru–P1	2.2940(8)	Cl1–Ru–P2	84.65(3)	Ru–N2	2.185(3)	Cl1–Ru–N1	87.00(6)	Ru1–N2	2.079(12)	Cl1–Ru1–N1	88.1(4)
Ru–P2	2.2923(8)	Cl1–Ru–O1	84.01(6)	Ru–P1	2.3290(8)	Cl1–Ru–N2	87.66(6)	Ru1–P1	2.299(4)	Cl1–Ru1–N2	166.1(3)
Ru–O1	2.209(2)	Cl2–Ru–S	93.65(3)	Ru–P2	2.3233(8)	Cl2–Ru–P1	97.48(3)	Ru1–P2	2.332(4)	Cl2–Ru1–P1	173.08(14)
S–O2	1.483(2)	Cl2–Ru–P1	89.38(3)	P1–C13	1.862(3)	Cl2–Ru–P2	89.74(3)	Ru2–Cl3	2.368(4)	Cl2–Ru1–P2	85.61(14)
P1–C13	1.832(3)	Cl2–Ru–P2	165.23(3)	P2–C24	1.832(3)	Cl2–Ru–N1	89.20(6)	Ru2–Cl4	2.450(4)	Cl2–Ru1–N1	80.5(4)
P2–C25	1.844(3)	Cl2–Ru–O1	85.88(6)			Cl2–Ru–N2	87.54(6)	Ru2–P4	2.317(4)	Cl2–Ru1–N2	89.1(4)
		P1–Ru–S	97.53(3)			P1–Ru–P2	96.09(3)	Ru2–P3	2.341(4)	P1–Ru1–P2	100.85(15)
		P2–Ru–S	97.12(3)			P1–Ru–N1	169.57(7)	Ru2–N4	2.140(14)	P1–Ru1–N1	93.1(4)
		O1–S–Ru	178.89(5)			P1–Ru–N2	92.35(7)	Ru2–N3	2.086(12)	P1–Ru1–N2	92.2(4)
		P1–Ru–P2	99.16(3)			P2–Ru–N1	91.92(7)			P2–Ru1–N1	166.0(4)
		P1–Ru–O1	81.47(6)			P2–Ru–N2	171.40(7)			P2–Ru1–N2	99.5(3)
		P2–Ru–O1	83.52(6)			N1–Ru–N2	79.89(10)			N1–Ru1–N2	78.0(4)
										Cl3–Ru2–P3	93.13(15)
										Cl3–Ru2–Cl4	88.81(14)
										N3–Ru2–N4	77.2(4)
										P3–Ru2–N4	166.1(4)
										P3–Ru2–N3	100.6(3)

As complexes **3** and **7** showed an excellent conversion rate in the initial studies, the catalytic activity of complex **3** was tested with a reduced catalytic loading of 0.01 mol %

under more strenuous conditions (pressure (H<sub>2</sub>) = 15 atm, *T* = 70 °C) in an attempt to achieve a high-turnover frequency (TOF). The conversion rate was monitored periodically by gas chromatography, and the results are displayed in Table 7 and graphically represented in Figure 8. The conversion of half of the styrene into ethylbenzene was observed within 40 min with a turnover frequency of

(17) Joshi, A. M.; MacFarlane, K. S.; James, B. R. *J. Organomet. Chem.* **1995**, 488, 161–167.

(18) Moldes, I.; de la Encarnacion, E.; Ros, J.; Alvarez-Larena, A.; Piniella, J. F. *J. Organomet. Chem.* **1998**, 566, 165–174.

**Table 5.** Selected Bond Distances (Å) and Bond Angles (deg) for Complexes **7** and **8**

complex <b>7</b>				complex <b>8</b>			
distance		angle		distance		angle	
Ru1–Cl1	2.4086(12)	Cl1–Ru1–Cl2	166.93(4)	Ru–Cl1	2.4340(9)	Cl1–Ru–Cl2	85.82(3)
Ru1–Cl2	2.3943(12)	Cl1–Ru1–P1	88.93(4)	Ru–Cl2	2.4858(9)	Cl1–Ru–P1	87.97(3)
Ru1–P1	2.3556(13)	Cl1–Ru1–P2	95.53(4)	Ru–P1	2.2921(9)	Cl1–Ru–P2	104.70(3)
Ru1–P2	2.3481(13)	Cl1–Ru1–P3	92.50(4)	Ru–P2	2.3314(8)	Cl1–Ru–O2	80.00(10)
Ru1–P3	2.2563(12)	Cl1–Ru1–O	85.94(8)	Ru–O2	2.160(3)	Cl1–Ru–N	167.71(8)
Ru1–O	2.235(3)	Cl2–Ru1–P1	85.77(4)	Ru–N	1.998(3)	Cl2–Ru–P1	171.86(3)
		Cl2–Ru1–P2	85.29(4)			Cl2–Ru–P2	87.46(3)
		Cl2–Ru1–P3	100.27(4)			Cl2–Ru–O2	81.16(10)
		Cl2–Ru1–O	81.33(8)			Cl2–Ru–N	93.75(9)
		P1–Ru1–P2	158.53(4)			P1–Ru–P2	99.22(3)
		P1–Ru1–P3	101.93(4)			P1–Ru–O2	92.59(10)
		P2–Ru1–P3	98.85(4)			P2–Ru–O2	167.38(10)
		P1–Ru1–O	79.10(9)			P1–Ru–N	91.19(9)
		P2–Ru1–O	80.28(9)			P2–Ru–N	87.53(8)
		P3–Ru1–O	178.13(9)			O2–Ru–N	87.79(12)

**Table 6.** Hydrogenation of Styrene Using Catalysts **1–5**, **7**, and **8**<sup>a</sup>

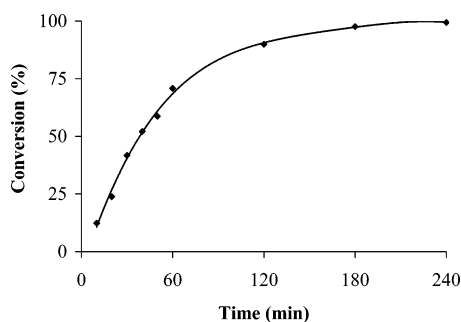
entry	catalyst	time (h)	conversion (%)
1	<b>1</b>	6	96.5
2	<b>2</b>	5	94.3
3	<b>3</b>	4	100
4	<b>4</b>	5	96.4
5	<b>5</b>	8	68.8
6	<b>6</b>	4	4.1
7	<b>7</b>	4	100
8	<b>8</b>	4	98.3

<sup>a</sup> Reagents and conditions: olefin (1.0 mmol), catalyst (0.1 mol %), pressure (H<sub>2</sub>) = 10 atm, THF (20 mL), 70 °C, stirring speed 400 rpm.

**Table 7.** Hydrogenation of Styrene Using Complex **3**<sup>a</sup>

entry	time (min)	conversion (%)	TOF (h <sup>-1</sup> )
1	10	12.3	7380
2	20	23.8	7140
3	30	41.7	8340
4	40	52.1	7815
5	50	58.7	7044
6	60	70.8	7080
7	120	89.9	4495
8	180	97.6	3253
9	240	99.4	2485

<sup>a</sup> Reagents and conditions: styrene (1.0 mmol), **3** (0.01 mol %), pressure (H<sub>2</sub>) = 15 atm, THF (30 mL), 70 °C, stirring speed 400 rpm.

**Figure 8.** Graphical representation of catalytic hydrogenation of styrene by using complex **3**.

78 15 h<sup>-1</sup> under these conditions. The reaction proceeds at a faster rate in the initial stage, and the rate gradually decreases with respect to time, which may be due to the decrease in the concentration of the substrate and also due to the partial decomposition of the catalyst. However, addition of 1.0 mmol of substrate into the reaction mixture increased the conversion rate but failed to show the full initial

activity. The catalytic activity was unaltered even in the presence of base.

## Conclusion

Several new ruthenium(II) complexes containing DPEphos in all possible coordination modes have been synthesized and are well characterized. The large bite angle DPEphos with a relatively rigid diphenyl ether backbone containing both oxygen and phosphorus donor sites offers different coordination modes and also behaves as a hemilabile ligand. The half-sandwich ruthenium(II) complex was prepared in excellent yield by interacting DPEphos directly with RuCl<sub>3</sub>·3H<sub>2</sub>O in the presence of cyclopentadiene. The bulkiness of the DPEphos ligand plays a key role in the formation of the specific isomeric product. In the mixed ligand Ru<sup>II</sup> complexes **3–7**, depending upon the steric nature of the environment, the DPEphos ligand offers different modes of coordination. In complex **3**, the DPEphos ligand binds with the ruthenium center in fac orientation, whereas upon substitution of the dmsoligand with PPh<sub>3</sub>, it isomerizes into the mer complex **7**. The complexes **4** and **6** are obtained as trans,cis isomers and **5** as the cis,cis isomer. Highly solvated complexes are utilized to make mixed ligand complexes with interesting binding properties. In many complexes, the oxygen atom of DPEphos binds to the metal center to provide temporary coordinative saturation until it is required to furnish the active site for the incoming substrates, an important feature in homogeneous catalysis which is thoroughly exploited by van Leeuwen and others. The complexes **3** and **7** show excellent catalytic activity in hydrogenation reactions. We are presently employing some of these ruthenium complexes in transfer hydrogenation reactions, and the work is in progress.

## Experimental Section

**Materials.** All manipulations were performed under an atmosphere of dry nitrogen using standard Schlenk techniques. All the solvents were purified by a conventional procedure<sup>19</sup> and distilled under nitrogen prior to use. The compounds DPEphos,<sup>7a</sup> cis-[RuCl<sub>2</sub>-(dmsol)<sub>4</sub>],<sup>20</sup> and [(η<sup>6</sup>-p-cymene)RuCl<sub>2</sub>]<sub>2</sub><sup>12</sup> were prepared according to published procedures. RuCl<sub>3</sub>·3H<sub>2</sub>O, PPh<sub>3</sub>, 2,2'-bipyridine, 4,4'-

(19) Armarego, W. L. F.; Perrin, D. D. *Purification of Laboratory Chemicals*, 4th ed.; Butterworth-Heinemann Linacre House: Oxford, U.K., 1996.



bipyridine, and cyclopentadiene were purchased from Lancaster and used as received. Pyridine was purchased from S.D Fine Chemicals and freshly distilled prior to use.

**Instrumentation.** The  $^1\text{H}$ ,  $^{13}\text{C}\{^1\text{H}\}$ , and  $^{31}\text{P}\{^1\text{H}\}$  NMR ( $\delta$  in ppm) spectra were recorded using a Varian 400 Mercury Plus spectrometer operating at the appropriate frequencies using TMS and 85%  $\text{H}_3\text{PO}_4$  as internal and external references, respectively. Microanalyses were performed on a Carlo Erba model 1112 elemental analyzer. The absorption spectra were recorded on a JASCO-V570 spectrophotometer. Electrospray ionization (EI) mass spectrometry experiments were carried out using a Waters Q-TOF micro-YA-105. Melting points were recorded using capillary tubes and are uncorrected. GC analyses were performed using a Perkin-Elmer Clarus 500 GC fitted with a packed column.

**Synthesis of  $[(\eta^5\text{-C}_5\text{H}_5)\text{RuCl}(\text{DPEphos})]$  (1).** A mixture of DPEphos (0.412 g, 0.765 mmol) and freshly distilled cyclopentadiene (0.5 mL) in absolute ethanol (20 mL) was added dropwise to a refluxing ethanol solution (30 mL) of  $\text{RuCl}_3 \cdot 3\text{H}_2\text{O}$  (0.1 g, 0.382 mmol). After 4 h, the reaction mixture was cooled to room temperature and then filtered and cooled to  $-30^\circ\text{C}$  to obtain red crystals of **1**. Yield: 72% (0.204 g, 0.275 mmol). Mp:  $>250^\circ\text{C}$ . UV-vis [ $\text{CH}_2\text{Cl}_2$ ,  $\lambda$ , nm, ( $\epsilon$ ,  $\text{cm}^{-1}\text{M}^{-1}$ ): 389 (3421), 289 (13 283), 243 (36 886).  $^1\text{H}$  NMR (400 MHz,  $\text{CDCl}_3$ ):  $\delta$  4.10 (s,  $\text{C}_5\text{H}_5$ , 5H), 7.11–7.39 (m, *Ph*, 28H).  $^{31}\text{P}\{^1\text{H}\}$  NMR (162 MHz,  $\text{CDCl}_3$ ):  $\delta$  42.4 (s). Anal. Calcd for  $\text{C}_{41}\text{H}_{33}\text{OP}_2\text{RuCl}$ : C, 66.53; H, 4.49. Found: C, 66.79; H, 4.55. MS (EI):  $m/z$  705.08 [ $\text{M} - \text{Cl}$ ] $^+$ .

**Synthesis of  $[(\eta^6\text{-}p\text{-cymene})\text{RuCl}_2]_2(\mu\text{-DPEphos})$  (2).** A solution of  $[(\eta^6\text{-}p\text{-cymene})\text{RuCl}_2]_2$  (0.050 g, 0.082 mmol) in  $\text{CH}_2\text{Cl}_2$  (5 mL) was added dropwise to a stirring solution of DPEphos (0.044 g, 0.082 mmol) also in  $\text{CH}_2\text{Cl}_2$  (10 mL) at room temperature. After 8 h, the reaction mixture was concentrated to 5 mL and diethyl ether (10 mL) was added to give red crystals of **2**. Yield: 87% (0.082, 0.071 mmol). Mp:  $>250^\circ\text{C}$ . UV-vis [ $\text{CH}_2\text{Cl}_2$ ,  $\lambda$ , nm, ( $\epsilon$ ,  $\text{cm}^{-1}\text{M}^{-1}$ ): 378 (3377), 293 (13 762), 242 (34 532).  $^1\text{H}$  NMR (400 MHz,  $\text{CDCl}_3$ )  $\delta$  1.16 (d, *ipr-CH* $_3$ ,  $^3J_{\text{HH}} = 7.2$  Hz, 6H), 1.80 (s, *p-CH* $_3$ , 3H), 2.87 (s, br, *ipr-CH*, 1H), 4.79 (d, 2H, *Ph-CH* $_2$ ,  $^3J_{\text{HH}} = 6.8$  Hz), 5.00 (d, *Ph-CH*, 2H), 6.77–7.93 (m, *Ph*, 56H).  $^{31}\text{P}\{^1\text{H}\}$  NMR (162 MHz,  $\text{CDCl}_3$ )  $\delta$  21.3 (s). Anal. Calcd for  $\text{C}_{56}\text{H}_{56}\text{OP}_2\text{Ru}_2\text{Cl}_4$ : C, 58.44; H, 4.90. Found: C, 58.40; H, 4.78.

**Synthesis of  $fac\text{-}[\text{RuCl}_2(\kappa^3\text{-}P, O, P\text{-DPEphos})(\text{dmsO})]$  (3).** A solution of  $cis\text{-}[\text{RuCl}_2(\text{dmsO})_4]$  (0.200 g, 0.413 mmol) in  $\text{CH}_2\text{Cl}_2$  (20 mL) was added dropwise to a solution of DPEphos (0.222 g, 0.413 mmol) in  $\text{CH}_2\text{Cl}_2$  (30 mL) at room temperature. The reaction mixture was stirred for 24 h. The clear yellow solution was concentrated to 10 mL and kept at room temperature for 3 days to afford yellow crystals of analytical purity. Yield: 82% (0.267 g, 0.339 mmol). Mp:  $228^\circ\text{C}$  (dec). UV-vis [ $\text{CH}_2\text{Cl}_2$ ,  $\lambda$ , nm, ( $\epsilon$ ,  $\text{cm}^{-1}\text{M}^{-1}$ ): 319 (2964), 261 (32 896), 244 (33 971).  $^1\text{H}$  NMR (400 MHz,  $\text{CDCl}_3$ ):  $\delta$  2.91 (s, *CH* $_3$ , 6H), 6.74–8.05 (m, *Ph*, 28H).  $^{31}\text{P}\{^1\text{H}\}$  NMR (162 MHz,  $\text{CDCl}_3$ ):  $\delta$  45.0 (s). Anal. Calcd for  $\text{C}_{38}\text{H}_{34}\text{O}_2\text{P}_2\text{RuSCl}_2$ : C, 57.87; H, 4.34; S, 4.07. Found: C, 57.84; H, 4.33; S, 3.98. MS (EI):  $m/z$  752.96 [ $\text{M} - \text{Cl}$ ] $^+$ .

**Synthesis of  $trans, cis\text{-}[\text{RuCl}_2(\text{DPEphos})(\text{C}_5\text{H}_5\text{N}_2)]$  (4).** A solution of pyridine (0.006 g, 0.076 mmol) in  $\text{CH}_2\text{Cl}_2$  (5 mL) was added dropwise to a solution of **3** (0.030 g, 0.038 mmol) in  $\text{CH}_2\text{Cl}_2$  (10 mL) at room temperature. The mixture was stirred for 12 h. The solution was concentrated to 5 mL and layered with petroleum ether (bp  $60\text{--}80^\circ\text{C}$ ) (5 mL) and kept at room temperature for 1 day to obtain a yellow crystalline solid. Yield: 71% (0.023 g, 0.027 mmol). Mp:  $>250^\circ\text{C}$ . UV-vis [ $\text{CH}_2\text{Cl}_2$ ,  $\lambda$ , nm, ( $\epsilon$ ,  $\text{cm}^{-1}\text{M}^{-1}$ ): 315

(5340), 241 (3331).  $^1\text{H}$  NMR (400 MHz,  $\text{CDCl}_3$ ):  $\delta$  6.80 (s, br, 6H,  $\text{C}_5\text{H}_5\text{N}$ ), 6.97–7.52 (m, br, *Ph*, 28H), 8.67 (s, br,  $\text{C}_5\text{H}_5\text{N}$ , 4H).  $^{31}\text{P}\{^1\text{H}\}$  NMR (162 MHz,  $\text{CDCl}_3$ ):  $\delta$  38.0 (s, br). Anal. Calcd for  $\text{C}_{46}\text{H}_{38}\text{OP}_2\text{RuN}_2\text{Cl}_2$ : C, 63.60; H, 4.41; N, 3.22. Found: C, 63.17; H, 4.61; N, 3.49. MS (EI):  $m/z$  754.03 [ $\text{M} - \text{C}_5\text{H}_5\text{N} \cdot \text{Cl}$ ] $^+$ .

**Synthesis of  $cis, cis\text{-}[\text{RuCl}_2(\text{DPEphos})(2,2'\text{-bipyridine})]$  (5).** A solution of 2,2'-bipyridine (0.006 g, 0.038 mmol) in  $\text{CH}_2\text{Cl}_2$  (5 mL) was added dropwise to a solution of **3** (0.030 g, 0.038 mmol) in  $\text{CH}_2\text{Cl}_2$  (10 mL) at room temperature. The mixture was stirred for 12 h, concentrated to 5 mL, and layered with petroleum ether (5 mL) to obtain a red crystalline solid. Yield: 90% (0.029 g, 0.034 mmol). Mp:  $>250^\circ\text{C}$ . UV-vis [ $\text{CH}_2\text{Cl}_2$ ,  $\lambda$ , nm, ( $\epsilon$ ,  $\text{cm}^{-1}\text{M}^{-1}$ ): 449 (3466), 302 (19 233), 242 (36 912).  $^1\text{H}$  NMR (400 MHz,  $\text{CDCl}_3$ ):  $\delta$  6.07 (m, *bpy*, 3H), 6.68–7.47 (m, *Ph*, 28H), 7.79 (d, *bpy*,  $^3J_{\text{HH}} = 7.2$  Hz, 1H), 7.94 (d, *bpy*,  $^3J_{\text{HH}} = 8.0$  Hz, 1H), 8.34 (d, *bpy*,  $^3J_{\text{HH}} = 6.0$  Hz, 1H), 9.05 (m, *bpy*, 1H).  $^{31}\text{P}\{^1\text{H}\}$  NMR (162 MHz,  $\text{CDCl}_3$ ):  $\delta$  37.0 (d,  $^2J_{\text{PP}} = 32.4$  Hz), 31.0 (d,  $^2J_{\text{PP}} = 31.1$  Hz). Anal. Calcd for  $\text{C}_{46}\text{H}_{36}\text{OP}_2\text{RuN}_2\text{Cl}_2$ : C, 63.74; H, 4.19; N, 3.23. Found: C, 63.44; H, 4.19; N, 3.30. MS (EI):  $m/z$  831.06 [ $\text{M} - \text{Cl}$ ] $^+$ .

**Synthesis of  $trans, cis\text{-}[\text{RuCl}_2(\text{DPEphos})(\mu\text{-}4,4'\text{-bipyridine})]_n$  (6).** A solution of 4,4'-bipyridine (0.006 g, 0.038 mmol) in  $\text{CH}_2\text{Cl}_2$  (5 mL) was added dropwise to a solution of **3** (0.030 g, 0.038 mmol) in  $\text{CH}_2\text{Cl}_2$  (10 mL) at room temperature. The mixture was stirred for 12 h to obtain a red precipitate which was filtered, washed with  $\text{Et}_2\text{O}$ , and dried under vacuum to afford the analytically pure compound **6**. Yield: 95% (0.031 g). Mp:  $>250^\circ\text{C}$ . UV-vis [ $\text{CH}_2\text{Cl}_2$ ,  $\lambda$ , nm, ( $\epsilon$ ,  $\text{cm}^{-1}\text{M}^{-1}$ ): 500 (5212), 395 (9827), 238 (39 857).  $^1\text{H}$  NMR (400 MHz,  $\text{CDCl}_3$ ):  $\delta$  6.79–7.45 (m, *Ph*, 28H), 7.56 (d, *bpy*,  $^3J_{\text{HH}} = 6.0$  Hz, 4H), 8.74 (d, *bpy*, 4H).  $^{31}\text{P}\{^1\text{H}\}$  NMR (162 MHz,  $\text{CDCl}_3$ ):  $\delta$  36.5 (s). Anal. Calcd for  $\text{C}_{46}\text{H}_{36}\text{OP}_2\text{RuN}_2\text{Cl}_2$ : C, 63.74; H, 4.19; N, 3.23. Found: C, 63.86; H, 4.21; N, 3.67.

**Synthesis of  $mer, trans\text{-}[\text{RuCl}_2(\kappa^3\text{-}P, P, O\text{-DPEphos})(\text{PPh}_3)]$  (7).** A solution of  $\text{PPh}_3$  (0.010 g, 0.038 mmol) in  $\text{CH}_2\text{Cl}_2$  (4 mL) was added dropwise to a solution of **3** (0.030 g, 0.038 mmol) in  $\text{CH}_2\text{Cl}_2$  (10 mL) at room temperature. After 12 h, the solution was concentrated to 3 mL and layered with petroleum ether to obtain a red crystalline solid. Yield: 78% (0.029 g, 0.030 mmol). Mp:  $220^\circ\text{C}$  (dec). UV-vis [ $\text{CH}_2\text{Cl}_2$ ,  $\lambda$ , nm, ( $\epsilon$ ,  $\text{cm}^{-1}\text{M}^{-1}$ ): 360 (7473), 286 (34 467), 238 (28 031).  $^1\text{H}$  NMR (400 MHz,  $\text{CDCl}_3$ ):  $\delta$  6.80–7.50 (m, *Ph*, 43H).  $^{31}\text{P}\{^1\text{H}\}$  NMR (162 MHz,  $\text{CDCl}_3$ ):  $\delta$  54.0 (t,  $\text{PPh}_3$ ,  $^2J_{\text{PP}} = 29.4$  Hz), 27.2 (d,  $2\text{P}$ ,  $^2J_{\text{PP}} = 28.9$  Hz). Anal. Calcd for  $\text{C}_{54}\text{H}_{43}\text{OP}_3\text{RuCl}_2$ : C, 67.04; H, 4.41; N, 1.61. Found: C, 65.58; H, 4.47; N, 1.98. MS (EI):  $m/z$  937.07 [ $\text{M} - \text{Cl}$ ] $^+$ .

**Synthesis of  $cis, cis\text{-}[\text{RuCl}_2(\text{DPEphos})(\text{CH}_3\text{CN})(\text{H}_2\text{O})]$  (8).** The mixture of  $[(\eta^6\text{-}p\text{-cymene})\text{RuCl}_2]_2$  (0.050 g, 0.082 mmol) and DPEphos (0.044 g, 0.082 mmol) was refluxed in moist acetonitrile (20 mL). After 4 h, the reaction mixture was concentrated and layered with diethyl ether (10 mL) to afford yellow crystals of **8**. Yield: 68% (0.029 g). Mp:  $160^\circ\text{C}$  (dec). UV-vis [ $\text{CH}_2\text{Cl}_2$ ,  $\lambda$ , nm, ( $\epsilon$ ,  $\text{cm}^{-1}\text{M}^{-1}$ ): 396 (3023), 248 (37 323).  $^1\text{H}$  NMR (400 MHz,  $\text{CDCl}_3$ ):  $\delta$  1.38 (s,  $\text{H}_2\text{O}$ , 2H), 2.03 (s,  $\text{CH}_3\text{CN}$ , 3H), 6.57–7.74 (m, *Ph*, 28H).  $^{31}\text{P}\{^1\text{H}\}$  NMR (162 MHz,  $\text{CDCl}_3$ ):  $\delta$  35.3 (d,  $^2J_{\text{PP}} = 31.1$  Hz), 27.2 (d,  $^2J_{\text{PP}} = 32.4$  Hz). Anal. Calcd for  $\text{C}_{54}\text{H}_{43}\text{OP}_3\text{RuCl}_2$ : C, 59.30; H, 4.32; N, 1.82. Found: C, 59.89; H, 4.11; N, 1.68. MS (EI):  $m/z$  699.07 [ $\text{M} - \text{Cl}_2$ ] $^+$ .

**X-ray Crystallography.** A crystal of each of the compounds **1–5**, **7**, and **8** suitable for X-ray crystal analysis was mounted in a CryoLoop with a drop of Paratone oil and placed in the cold nitrogen stream of the Kryoflex attachment of the Bruker APEX CCD diffractometer. A full sphere of data for each crystal was collected using 606 scans in  $\omega$  ( $0.3^\circ$  per scan) at  $\phi = 0$ , 120, and

(20) Evans, I. P.; Spencer, A.; Wilkinson, G. *J. Chem. Soc., Dalton Trans.* **1973**, 204–209.



240° using the SMART software package.<sup>21</sup> The raw data were reduced to  $F^2$  values using the SAINT+ software,<sup>22</sup> and global refinement of unit cell parameters using ca. 4000–8000 reflections chosen from the full data sets was performed. Multiple measurements of equivalent reflections provided the basis for empirical absorption corrections as well as corrections for any crystal deterioration during the data collection (SADABS).<sup>23</sup> The structures were solved by direct methods (for **1**, **2**, **5**, and **7**), or the position of the metal atoms was obtained from a sharpened Patterson function (for **3**, **4**, and **8**) and refined by full-matrix least-squares procedures using the SHELXTL program package.<sup>24</sup> Hydrogen atoms were placed in calculated positions and included as riding contributions with isotropic displacement parameters tied to those of the attached non-hydrogen atoms.

**General Procedure for Catalytic Hydrogenation of Styrene.**

A mixture of Ru<sup>II</sup> complex (0.1 mol %), olefin (1.0 mmol), and 20 mL of THF was introduced to a 50 mL glass vessel. The glass vessel containing the reaction mixture was placed in the steel autoclave, and the reactor was sealed. The vessel was purged three

times with hydrogen, and then the autoclave was pressurized with 10 or 15 atm of hydrogen. The reaction mixture was stirred at 70 °C, and the progress of the reaction was determined by periodic GC analysis.

**Acknowledgment.** We are grateful to the Department of Science and Technology (DST), New Delhi, for funding through Grant SR/S1/IC-05/2003. We also thank the Department of Chemistry Instrumentation Facilities, IIT Bombay, and the Sophisticated Analytical Instrument Facility (SAIF), IIT Bombay, for spectral and analytical data. R.V. is thankful to IIT Bombay for JRF and SRF Fellowships. J.T.M. thanks The Louisiana Board of Regents through Grant LEQSF-(2002-03)-ENH-TR-67 for the purchase of the CCD diffractometer and the Chemistry Department of Tulane University for support of the X-ray laboratory. We are thankful to the referees for their valuable suggestions during the revision of this manuscript.

**Supporting Information Available:** X-ray crystallographic files in CIF format for the structure determinations of **1–5**, **7**, and **8**. This material is available free of charge via the Internet at <http://pubs.acs.org>.

IC061782L

- 
- (21) SMART, version 5.625; Bruker-AXS: Madison, WI, 2000.  
(22) INT+, version 6.35A; Bruker-AXS: Madison, WI, 2002.  
(23) Sheldrick, G. M. SADABS, version 2.05; University of Gottingen: Gottingen, Germany, 2002.  
(24) (a) SHELXTL, version 6.10; Bruker-AXS: Madison, WI, 2000. (b) Sheldrick, G. M. SHELXS97 and SHELXL97; University of Gottingen: Gottingen, Germany, 1997.